

Coordination of hamstrings is individual specific and is related to motor performance

Simon Avrillon, Gaël Guilhem, Aude Barthelemy, François Hug

▶ **To cite this version:**

Simon Avrillon, Gaël Guilhem, Aude Barthelemy, François Hug. Coordination of hamstrings is individual specific and is related to motor performance. Journal of Applied Physiology, 2018, 125 (4), pp.1069-1079. 10.1152/japplphysiol.00133.2018 . hal-02983807

HAL Id: hal-02983807

https://insep.hal.science//hal-02983807

Submitted on 30 Oct 2020

HAL is a multi-disciplinary open access archive for the deposit and dissemination of scientific research documents, whether they are published or not. The documents may come from teaching and research institutions in France or abroad, or from public or private research centers.

L'archive ouverte pluridisciplinaire **HAL**, est destinée au dépôt et à la diffusion de documents scientifiques de niveau recherche, publiés ou non, émanant des établissements d'enseignement et de recherche français ou étrangers, des laboratoires publics ou privés.

Coordination of hamstrings is individual-specific and is related to motor performance

Simon AVRILLON[1], Gaël GUILHEM[1*], Aude BARTHELEMY[1], François HUG[2,3,4]

[1] French Institute of Sport (INSEP), Research Department, Laboratory Sport, Expertise and Performance (EA 7370) Paris, France

[2] University of Nantes, Faculty of Sport Sciences, Laboratory Movement, Interactions, Performance (EA 4334), Nantes, France

[3] Institut Universitaire de France (IUF), Paris, France

[4] The University of Queensland, Centre for Clinical Research Excellence in Spinal Pain, Injury and Health, School of Health and Rehabilitation Sciences, Brisbane, Australia

[*]**Correspondence and reprints:**
Gaël Guilhem, PhD
Institut National du Sport, de l'Expertise et de la Performance
Département de la Recherche
Laboratoire Sport, Expertise et Performance (EA 7370)
11, avenue du Tremblay
75012 Paris
France
Tel: +33 (0)1 41 74 43 36
Fax: +33 (0)1 41 75 45 35
e-mail: gael.guilhem@insep.fr

Running title: Hamstring coordination and performance

Downloaded from www.physiology.org/journal/jappl by ${individualUser.givenNames} ${individualUser.surname} (109.007.033.126) on August 30, 2018.
Copyright © 2018 American Physiological Society. All rights reserved.

ABSTRACT (247 words)

The torque sharing strategies between synergist muscles may have important functional consequences. This study involved two experiments. The first experiment (n=22) aimed: i) to determine the relationship between the distribution of activation and the distribution of torque-generating capacity among the heads of the hamstring, and ii) to describe individual torque-sharing strategies and to determine whether these strategies are similar between legs. The second experiment (n=35) aimed to determine whether the distribution of activation between the muscle heads affects the endurance performance during a sustained submaximal knee flexion task. Surface electromyography (EMG) was recorded from biceps femoris (BF), semimembranosus (SM), and semitendinosus (ST) during submaximal isometric knee flexions. Torque-generating capacity was estimated by measuring muscle volume, fascicle length, pennation angle and moment arm. The product of the normalized EMG amplitude and the torque-generating capacity was used as an index of muscle torque. The distributions of muscle activation and of torque-generating capacity were not correlated significantly (all $P>0.18$). Thus, there was a torque imbalance between the muscle heads (ST torque > BF and SM torque; $P<0.001$), the magnitude of which varied greatly between participants. A significant negative correlation was observed between the imbalance of activation across the hamstring muscles and the time to exhaustion ($P<0.001$), i.e. the larger the imbalance of activation across muscles, the lower the muscle endurance performance. Torque-sharing strategies between the heads of the hamstrings are individual-specific and related to muscle endurance performance. Whether these individual strategies play a role in hamstring injury remains to be determined.

NEW & NOTEWORTHY:

Downloaded from www.physiology.org/journal/jappl by ${individualUser.givenNames} ${individualUser.surname} (109.007.033.126) on August 30, 2018.
Copyright © 2018 American Physiological Society. All rights reserved.

- The distribution of activation among the heads of the hamstring is not related to the distribution of torque-generating capacity.
- The torque-sharing strategies within hamstring muscles vary greatly between individuals but are similar between legs.
- Hamstring coordination affects endurance performance; i.e. the larger the imbalance of activation across the muscle heads, the lower the muscle endurance.

KEYWORDS:

Hamstring; Individual coordination; Muscle torque; Muscle endurance

Downloaded from www.physiology.org/journal/jappl by ${individualUser.givenNames} ${individualUser.surname} (109.007.033.126) on August 30, 2018.
Copyright © 2018 American Physiological Society. All rights reserved.

1. INTRODUCTION

Muscle coordination is defined as the distribution of muscle force/torque (rather than just activation) among individual muscles to produce a given motor task (15). As the number of muscles exceeds the dimensionality of most tasks, many different coordination strategies are *theoretically possible* to achieve the same goal. In this way, Hug and Tucker (15) hypothesized that each individual has unique muscle coordination strategies that will have specific mechanical effects on his/her musculoskeletal system. To test this hypothesis, it is necessary to consider the torque produced by individual muscles instead of activation alone.

Muscle torque depends on both the muscle activation and several biomechanical factors (e.g., physiological cross-sectional area [PCSA], specific tension, moment arm, and force–length and force–velocity relationships). When considering muscles with similar specific tension during an isometric task, an index of torque can be estimated from the muscle activation, PCSA and moment arm. Using this approach, Hug et al. (14) highlighted large interindividual differences in the balance of force between the *vastus lateralis* (VL) and the *vastus medialis* (VM). Specifically, during an isometric knee extension at 20% of the maximal voluntary contraction (MVC), the VL/VM ratio of the index of force ranged from 38.4 to 84.0%. This variability resulted from individual differences in both muscle activation and PCSA.

The balance of torque between synergist muscles may have important functional consequences. For example, using an indirect index of muscle activity (functional Magnetic Resonance Imaging [fMRI]), Schuermans et al. (34, 35) highlighted the possible role of altered coordination between the heads of the hamstring in risk of injury. Interestingly, a large inter-individual variability in PCSA of individual heads of the hamstring has been observed both in cadavers (coefficient of variation [CV]: 33.3% [biceps femoris short head, BFsh] to 42.4% [biceps femoris long head, BFlh] (42)) and active people (CV: 40.6% for BFlh (36)). It is unknown whether muscle activation and/or muscle moment arm counteract these individual

Downloaded from www.physiology.org/journal/jappl by ${individualUser.givenNames} ${individualUser.surname} (109.007.033.126) on August 30, 2018.
Copyright © 2018 American Physiological Society. All rights reserved.

differences in PCSA such that the distribution of torque among the muscle heads is similar between individuals.

In addition to their possible role in the risk of injury, muscle coordination strategies might impact muscle performance, as was suggested indirectly by Schuermans et al. (34, 35). Let us consider two synergist muscles (A and B) during a sustained isometric task at 20% MVC maintained until exhaustion. During such a task, the muscle endurance performance can be estimated by the time to exhaustion (16). There are two scenarios for the distribution of activation during this task: i) A and B are both activated at about 20% of their maximal activation, i.e. activation is equally shared between muscles, or ii) there is an imbalanced activation between A and B, in which case one muscle will necessarily be activated at a higher level than that requested by the task, e.g., A is activated at 30% and B at 10%. In the latter case, and in the absence of substantial change in activation strategy during the task, it is likely that muscle A would develop fatigue earlier and this, in turn, would lead to a shorter time to exhaustion, reflective of lower performance.

This study involved two experiments. The aims of the first experiment were: i) to determine the relationship between the distribution of activation and the distribution of torque-generating capacity among the heads of the hamstring, and ii) to describe individual torque-sharing strategies and to determine whether these strategies are similar between legs. To address these two aims, muscle activation was estimated using electromyography (EMG) during submaximal isometric knee flexion tasks at 20% of MVC. The between-day reliability of the activation distribution between the muscle heads was first assessed to test the robustness of the activation strategies. Muscle torque-generating capacity was estimated by measurements of the muscle PCSA and moment arm. The second experiment aimed to determine whether the distribution of activation between the muscle heads affects the endurance performance during a sustained submaximal task.

Downloaded from www.physiology.org/journal/jappl by ${individualUser.givenNames} ${individualUser.surname} (109.007.033.126) on August 30, 2018.
Copyright © 2018 American Physiological Society. All rights reserved.

2. METHODS

2.1. Participants

Twenty-two healthy volunteers (age 24 ± 2 yr, weight 65 ± 10 kg, height 173 ± 8 cm; 11 females/11 males) participated in experiment I. In addition to these 22 participants, 13 additional participants were included in experiment II such that a total of 35 healthy volunteers participated in experiment II (age 24 ± 3 yr, weight 66 ± 11 kg, height 173 ± 9 cm; 16 females/19 males). Participants had no history of hamstring strain injury. The experimental procedures were approved by the local ethics committee (approval reference no. 3418, RCB no. 2016-A00715-46), and all procedures adhered to the Declaration of Helsinki.

2.2. Assessment of muscle activation

2.2.1. Experimental setup

For *experiment I*, participants attended two identical testing sessions to assess the between-day reliability of the activation of the hamstring muscles (i.e., semitendinosus [ST], semimembranosus [SM], BFlh). Participants sat on an isokinetic dynamometer (Con-trex, CMV AG, Dübendorf, Switzerland) with non-compliant straps placed around the chest, the pelvis and the thigh. The hip and the knee were flexed at angles of 90° and 45°, respectively (0° = neutral position for the hip and full extension for the knee). The 45° angle for the knee was chosen because it represents the angle at which the maximal knee flexion torque can be generated, i.e. the optimal angle (19). Visual feedback of the exerted torque signal was provided to the participant on a screen. The experimental setup used for *experiment II* was identical to that described above.

2.2.2. Mechanical data

Downloaded from www.physiology.org/journal/jappl by ${individualUser.givenNames} ${individualUser.surname} (109.007.033.126) on August 30, 2018.
Copyright © 2018 American Physiological Society. All rights reserved.

The torque signal from the isokinetic dynamometer was recorded and digitized by a USB data acquisition module (DT9804; Data Translation, Marlboro, MA, USA) at 1000 Hz. Torque was corrected for gravity and low-pass filtered at 20 Hz using a third-order Butterworth filter.

2.2.3. Surface electromyography

Myoelectric activity was recorded bilaterally with surface electrodes placed over the semitendinosus (ST), semimembranosus (SM) and biceps femoris (BF). Participants were seated on a customized piece of foam with a free space beneath each muscle to ensure that there was no contact between the electrodes and the seat. We used B-mode ultrasound (Aixplorer v11, Supersonic Imagine, Aix-en-Provence, France) to determine the appropriate placement for the ST, SM, and BF electrodes, longitudinally with respect to the muscle fascicle's alignment and away from the borders of the neighboring muscles. The superficial part of the BFsh is close to the popliteal fossa, so it was not possible to investigate this muscle. Therefore, we followed the SENIAM recommendation for electrode placement on the BF and considered the recorded myoelectrical activity originating from this pair of electrodes as being representative of both the short and the long heads (10). The skin was shaved and then cleaned with alcohol, and a pair of Ag/AgCl electrodes (Blue sensor N-00-S, Ambu, Copenhagen, Denmark) was attached to the skin with an inter-electrode distance of 20 mm (center-to-center). Raw EMG signals were pre-amplified 1000 times, band-pass filtered (10–500 Hz, third-order Butterworth filter) and sampled at 2000 Hz (Zerowire, Aurion, Milan, Italy). EMG and mechanical data were synchronized using a transistor–transistor logic pulse.

2.2.4. Experimental tasks

After a standardized warm-up (10 and 5 isometric contractions at 50% and 80% of maximal perceived intensity, respectively; 2 s hold and 2 s rest), participants performed three maximal

Downloaded from www.physiology.org/journal/jappl by ${individualUser.givenNames} ${individualUser.surname} (109.007.033.126) on August 30, 2018.
Copyright © 2018 American Physiological Society. All rights reserved.

voluntary knee flexions. Each contraction was maintained for 3 to 5 s; contractions were separated by a 120-s rest period. The maximal value obtained from a moving average window of 300 ms was considered as the peak flexion torque. Using visual feedback, participants then performed three 10-s isometric knee flexions at 20% of MVC torque separated by 30 s of rest. *Experiment I* stopped at this point, but *experiment II* included a second part in which the time to exhaustion was measured. Specifically, after a 5-min rest period, participants performed an isometric knee flexion at 20% of MVC torque until task failure. They were strongly encouraged to maintain the torque as long as possible. Task failure was defined as the moment when the torque they produced decreased by more than 5% of the target level for at least 3 s. This task was performed with each leg, in a randomized order and separated by 5 min of rest.

2.2.5. Data processing

All mechanical and EMG data were analyzed using MATLAB (R2017a, The Mathworks, Nathick, MA, USA). To determine the maximal EMG amplitude, the Root Mean Square (RMS) of the EMG signal was calculated over a moving time window of 300 ms and the maximal value was considered as the maximal activation level. During the submaximal isometric knee flexions, the RMS EMG amplitude was calculated over 5 s at the time period corresponding to the lowest standard deviation of the torque signal. Then, this value was normalized to that measured during the MVC tasks. The ratio of activation between the hamstring muscles was calculated as the normalized RMS EMG of the considered muscle divided by the sum of normalized RMS EMG values of all three muscles.

2.3. Estimation of torque-generating capacity

2.3.1. Magnetic resonance imaging (MRI)

Downloaded from www.physiology.org/journal/jappl by ${individualUser.givenNames} ${individualUser.surname} (109.007.033.126) on August 30, 2018.
Copyright © 2018 American Physiological Society. All rights reserved.

Both muscle volume and moment arm were estimated through Magnetic Resonance Imaging (MRI; 1.5 T, Intera Achieva, Philips, Amsterdam, Netherlands). Participants were first placed in supine position with their knees flexed at 45°, i.e., the same knee angle as that used for the experimental tasks. Flexible surface coils (SENSE, Philips , Amsterdam, Netherlands) were strapped to the medial and lateral sides of the knee. A volumetric sequence (3D T1 fast field echo, 5.17 min, FOV 250 mm × 179 mm, TR/TE = 24/11.5 ms, voxel size: 1 × 1 × 2 mm, flip angle: 50°) allowed an anatomical zone from half of the femur to half of the tibia to be imaged. This sequence was used to measure the moment arm. For each muscle, the knee flexion moment arm was defined as the shortest distance between the rotation center of the knee joint and the line of action of the considered muscle. To begin, the femoral condyle was segmented manually using 3D medical image processing software (Mimics, Materialise, Leuven, Belgium). The 3D coordinates of the lateral and medial femoral epicondyles were determined, and the center of the joint was calculated as the midpoint between these two points (5). Then, the distal part of the hamstring muscle-tendon unit (ST, SM, BF) was outlined (Fig. 1A). The centroid of the axial slices was calculated to reconstruct a line passing through, i.e. the musculotendon path. Finally, the perpendicular distance between the center of the joint and the musculotendon path was considered to be the moment arm. Due to their anatomical convergence, the distal tendon of the BFsh cannot be distinguished accurately from that of the BFlh (44). Consequently, we considered one common moment arm for both muscle heads, as has been done in other anatomical studies (37, 41).

A second acquisition sequence was dedicated to the measurement of the muscle volume. The participants were in a supine position, lying with their hips and knees fully extended. A spine coil (15 elements, SENSE, Philips) was placed under the pelvis and lower limbs to perform a volumetric sequence (3D T1 turbo fast field echo, 13.10 min, FOV 360 mm × 220 mm, TR/TE = 14/6.9 ms, voxel size: 0.8 × 0.8 × 2 mm, flip angle: 20°). Slice thickness was 2 mm

Downloaded from www.physiology.org/journal/jappl by ${individualUser.givenNames} ${individualUser.surname} (109.007.033.126) on August 30, 2018.
Copyright © 2018 American Physiological Society. All rights reserved.

without an inter-slice gap. Contiguous MR images were acquired from the iliac crest to half of the tibia to get images the hamstring heads (ST, SM, BFlh and BFsh), between their proximal and distal insertions. MR images of the ST, SM, BFlh and BFsh were segmented manually (Fig. 1B)

2.3.2. B-mode ultrasound

The field of view of the ultrasound transducer was too narrow (i.e., 42 mm) to image entire hamstring fascicles, which are typically longer than 12 cm for BFlh (44). To overcome this technical limitation, we used the built-in panoramic mode of the ultrasound device (Aixplorer V11, Supersonic Imagine). This mode uses an algorithm that fits a series of images, allowing the entire fascicles to be scanned within one continuous scan. The advantage of this approach over classical measurements from one B-mode image is that it does not require extrapolating the non-visible part of the fascicle (1). Participants were lying with the same hip and knee angles that were used during the submaximal task. The leg was attached to the dynamometer arm with a non-compliant strap. An ultrasound transducer (2–10 MHz, SL10-2, Supersonic Imagine, Aix-en-Provence, France) was placed over the muscle of interest and cross-sectional images were acquired in the longitudinal plane of the muscle to determine the path of the transducer. Scans began at the proximal insertion following the fascicle's plane in such a way that superficial and deep aponeuroses were visible. Scans progressed along the midline of the muscle until reaching the distal portion, at approximately at 90% of the femur length. The total scan time was 10 to 15 s. This was repeated for each muscle until two images with visible fascicles were obtained (Fig. 1C). A segmented line (with a spline fit) was used to model the fascicle and measure its length (ImageJ v1.48, National Institutes of Health, Bethesda, MD, USA). For the SM and BFlh, one fascicle was measured distally, medially, and proximally. The pennation angle was measured as the angle between the deep

Downloaded from www.physiology.org/journal/jappl by ${individualUser.givenNames} ${individualUser.surname} (109.007.033.126) on August 30, 2018.
Copyright © 2018 American Physiological Society. All rights reserved.

aponeurosis and the fascicle. Then, the three values were averaged to get a representative value for the entire muscle. As the BFsh images were shorter, one or two fascicles were measured for each participant. The ST muscle is fusiform, and, therefore, its fascicle length was considered to be the distance between the distal and proximal insertions as determined using the MR images.

2.3.3. Estimation of torque-generating capacity

PCSA of SM, BFlh and BFsh was calculated as follows (22):

$$\text{PCSA} = \frac{\text{Muscle volume}}{\text{Fascicle length}} \times \text{cosine(Pennation angle)}$$

where PCSA is expressed in cm^2, muscle volume in cm^3, and fascicle length in cm. Note that the fascicle length and pennation angle were assessed near the isometric optimal knee angle (45°; 0° = full extension of the knee). As ST muscle is fusiform, its PCSA was calculated as the ratio of the volume of the muscle to its length. For the head of each muscle, the product of PCSA with the moment arm (m) was considered as an index of torque-generating capacity. The ratio of torque-generating capacity between the hamstring muscles was calculated as the torque-generating capacity of the considered muscle divided by the sum of the torque-generating capacity of all three muscles.

2.4. Estimation of an index of muscle torque

During an isometric contraction, the difference of force produced by synergist muscles depends mainly on their PCSA, their activation, and their specific tension. Because hamstring muscles have similar fiber-types composition (9), and because the contractions were performed at low intensity during which it was likely that only slow fibers were recruited, specific tension was not expected to vary greatly between the muscle heads. Therefore, an index of muscle torque was calculated as follows:

Downloaded from www.physiology.org/journal/jappl by ${individualUser.givenNames} ${individualUser.surname} (109.007.033.126) on August 30, 2018.
Copyright © 2018 American Physiological Society. All rights reserved.

Index of muscle torque = PCSA × moment arm × normalized RMS EMG

where the index of muscle torque is expressed in arbitrary units (au), PCSA in cm^2, moment arm in m and normalized RMS EMG in percentage of RMS EMG_{max}. As was done for EMG and PCSA, we calculated the ratios of torque, i.e. BF/Hams, ST/Hams, and SM/Hams.

2.5. Statistics

Statistical analyses were performed using Statistica (v8, Statsoft, Tulsa, OK, USA). Distributions consistently passed the Kolmogorov–Smirnov normality test, and all data are reported as mean ± SD. The intra-class correlation coefficient (ICC) and the typical error were calculated to determine the robustness of EMG data between the testing sessions. EMG amplitude were compared for muscles and legs using separate repeated-measures ANOVAs (within-subject factors: leg [dominant, non-dominant] and muscle [ST, SM, BF]). Fascicle length, pennation angle, muscle volume, moment arm and torque-generating capacity were compared for muscles and legs using separate repeated-measures ANOVAs (within-subject factors: leg [dominant, non-dominant] and muscle [ST, SM, BFsh, BFlh]). When the sphericity assumption was violated in repeated ANOVAs (Mauchly's test), the Geisser–Greenhouse correction was used. When appropriate, post-hoc analyses were performed using Bonferroni tests.

To address the first aim (*experiment I*), the relationship between the distribution of activation and the distribution of torque-generating capacity among the heads of the hamstring was assessed using Pearson's correlation coefficient. To address the second aim (*experiment I*), we compared each torque ratio (ST/Hams, SM/Hams, BF/Hams) for legs using a paired *t*-test. Also, we tested the correlation between sides using Pearson's correlation coefficient. To address the third aim (*experiment II*), we first tested whether activation strategies changed during the sustained contraction by assessing the variability of the ratios of activation during

Downloaded from www.physiology.org/journal/jappl by ${individualUser.givenNames} ${individualUser.surname} (109.007.033.126) on August 30, 2018.
Copyright © 2018 American Physiological Society. All rights reserved.

the fatiguing task using both the coefficient of variation and the typical error. The imbalance of the activation among the three muscle heads was assessed by calculating the standard deviation of their RMS EMG amplitude measured during the 10-s submaximal knee flexion tasks; i.e., the higher the standard deviation, the larger the activation difference between the muscles. The level of significance was set at $P < 0.05$. We report a correlation of 0.5 as large, 0.3 as moderate, and 0.1 as small (7).

3. RESULTS

3.1. Experiment I

The torque measured during the maximal isometric knee flexion tasks was significantly higher for the dominant leg than for the non-dominant leg. The values averaged between the two sessions were 98.1 ± 33.2 Nm and 88.5 ± 29.4 Nm ($P < 0.001$).

3.1.1. Muscle activation

The between-day reliability of the normalized EMG amplitude measured during the submaximal isometric contraction at 20% MVC was fair to excellent (Table 1). ICC values ranged from 0.45 to 0.85 and the typical error ranged from 2.2% to 3.2% of RMS EMG_{max}. Although the reliability was good for both legs, activation of the muscles in the dominant leg appeared to be slightly more reliable (Table 1). For the specific purpose of this article, we focused on the distribution of activation among the muscle heads by calculating the activation ratios, i.e. BF/Hams, ST/Hams, and SM/Hams. The inter-day reliability was good to excellent for all of these ratios except for the ST/Hams ratio for the non-dominant leg, which exhibited an ICC value slightly lower than 0.60 (Table 2). ICC values ranged from 0.57 to 0.88, and the typical error ranged from 2.7% to 5.6%. Considering this overall good reliability, EMG data were averaged between days for further analysis.

Downloaded from www.physiology.org/journal/jappl by ${individualUser.givenNames} ${individualUser.surname} (109.007.033.126) on August 30, 2018.
Copyright © 2018 American Physiological Society. All rights reserved.

No differences in activation ratio were observed between legs (P = 0.34, P = 0.83, and P = 0.99 for BF/Hams, SM/Hams, and ST/Hams, respectively). The similarity was further confirmed by the large correlation coefficients between legs (r = 0.75 [P < 0.001], 0.55 [P = 0.008], and 0.68 [P < 0. 001] for BF/Hams, SM/Hams, and ST/Hams, respectively). Notably, the activation ratios were highly variable between participants (Fig. 2A). For example, when considering the dominant leg, the ratio of activation ranged from 19.9 to 48.1% for BF/Hams, from 23.7 to 56.8% for SM/Hams and from 17.0 to 43.4% for ST/Hams.

3.1.2. Torque-generating capacity

Architectural characteristics of each head of the hamstring muscle and the associated statistics are presented in Table 3. For the sake of clarity, we only report the statistics associated with torque-generating capacity, which relates to the first aim of this study. There was no main effect of the leg (P = 0.73) or the leg × muscle interaction (P = 0.50) on the torque-generating capacity. The absence of differences among the legs was further confirmed by the moderate to large correlation coefficients (r = 0.39 [P = 0.07], 0.44 [P = 0.038], and 0.72 [P < 0.001] for BF/Hams, SM/Hams, and ST/Hams, respectively). However, we observed a main effect of muscle (P < 0.001). More precisely, the torque-generating capacity of ST was significantly lower than that of BF (-41.3 ± 18.2%; P < 0.001) and SM (-44.3 ± 17.3%; P < 0.001). As reported for the ratios of activation, a large variability between individuals was observed (Fig. 2B). When considering the dominant leg, the ratio of torque-generating capacity ranged from 30.0 to 46.9% for BF/Hams, from 32.9 to 50.6% for SM/Hams, and from 11.9 to 34.6% for ST/Hams.

3.1.3. Relationship between activation and torque-generating capacity

Downloaded from www.physiology.org/journal/jappl by ${individualUser.givenNames} ${individualUser.surname} (109.007.033.126) on August 30, 2018.
Copyright © 2018 American Physiological Society. All rights reserved.

There was no significant correlation between the ratio of muscle activation and the ratio of torque-generating capacity, regardless of the muscle and the leg that were considered (dominant leg: r = 0.20 [P = 0.36], r = 0.03 [P = 0.90] and r = -0.31 [P = 0.16] for BF/Hams, SM/Hams and ST/Hams, respectively; non-dominant leg: r = 0.00 [P = 0.99], r = -0.02 [P = 0.91] and r = -0.14 [P = 0.54] for BF/Hams, SM/Hams and ST/Hams, respectively). These results indicate that the imbalance of torque-generating capacity observed between the muscle heads was neither counteracted nor accentuated by activation. This contributed to an imbalance of the torque index, the magnitude of which varied greatly between participants.

3.1.4. Torque-sharing strategies

When considering the torque index, which was calculated as the product of torque-generating capacity and the normalized EMG amplitude measured during the submaximal knee flexion, there was neither a main effect of the leg (P = 0.36) nor the muscle × leg interaction (P = 0.51). However, a main effect of muscle was found (P < 0.001). Specifically, the torque index of ST (7.0 ± 2.8 [au]) was lower than that of BF (13.7 ± 6.4; P < 0.001) and SM (16.1 ± 6.1; P < 0.001). There were no significant differences between BF and SM (P = 0.19). When considering the dominant leg, the torque index ratio reached 18.5 ± 6.8% for ST/Hams, 37.7 ± 10.1% for BF/Hams, and 43.8 ± 9.9% for SM/Hams (Fig. 3A). There was a significant correlation between the torque index ratios of the dominant and non-dominant legs for ST/Hams (r = 0.63 [P = 0.002]), BF/Hams (r = 0.60 [P = 0.003]) and SM/Hams (r = 0.48 [P = 0.025]) (Fig. 3B). The group distribution of the torque index ratios displayed in Fig. 3 reveals a large inter-individual variability.

3.2. Experiment II

Downloaded from www.physiology.org/journal/jappl by ${individualUser.givenNames} ${individualUser.surname} (109.007.033.126) on August 30, 2018.
Copyright © 2018 American Physiological Society. All rights reserved.

When considering the dominant leg, the coefficient of variation of the activation ratios measured during the limit time to exhaustion was low, i.e., 9.4% for ST/Hams, 9.5% for SM/Hams, and 11.4% for BF/Hams. The typical error (TE) was 5.7% for ST/Hams, 4.5% for SM/Hams, and 5.1% for BF/Hams. Similar values were reported for the non-dominant leg (CV: 7.4%, 10.6%, and 12.8%; TE: 2.9%, 6.3%, and 6.9% for ST/Hams, SM/Hams and BF/Hams, respectively). Therefore, we concluded that the activation strategies did not change drastically during the sustained submaximal contraction. The mean standard deviation of the RMS EMG amplitude measured during the 10-s contractions that preceded the sustained contraction was 3.2 ± 1.9% of RMS EMG_{max} (range: 0.4–8.3%) and 3.1 ± 1.6% of RMS EMG_{max} (range: 0.6–7.2%) for the dominant and non-dominant legs, respectively. Participants maintained the targeted torque for 466 ± 190 s (range: 195–1037 s) with their dominant legs and for 473 ± 210 s (range: 163–1260 s) with their non-dominant legs. There was a significant negative correlation between the standard deviation values and the time to exhaustion (r = -0.52 [P < 0.001] and r = -0.42 [P = 0.011] for the dominant and non-dominant legs, respectively) (Fig. 4). These correlations indicate that the larger the activation difference between the muscle heads, the shorter the time to exhaustion.

Downloaded from www.physiology.org/journal/jappl by ${individualUser.givenNames} ${individualUser.surname} (109.007.033.126) on August 30, 2018.
Copyright © 2018 American Physiological Society. All rights reserved.

4. DISCUSSION

Three novel findings resulted from this study. First, there was no correlation between the distribution of activation between the heads of the hamstring and the distribution of torque-generating capacity. Secondly, the torque-sharing strategy varied greatly between participants but it was similar for the participants' two legs. Thirdly, the larger the imbalance of activation across the muscle heads, the lower the muscle endurance. These results provide a deeper understanding of the interplay between the activation a muscle receives and its mechanical characteristics. By demonstrating a relationship between activation strategies and endurance performance, our findings also provide the foundation for future work to explore the roles of different muscle coordination strategies in motor performance. These results may have clinical relevance as they provide a basis for considering muscle coordination strategies as an intrinsic risk factor for hamstring strain injury.

4.1. Individual muscle activation strategies

When the entire sample of participants was considered, the activation ratios were similar for different muscles, which might lead to the conclusion that the activation is shared roughly equally among the three heads. However, inspection of the data for individual participants revealed a large variability, as illustrated by the SM/Hams ratio, which ranged from 23.7% to 56.8% (Fig. 2A). Large individual differences in EMG amplitude ratio already have been reported for knee extensors (14) and ankle plantar flexors (21). For example, Hug et al. (14) reported a VL/VM activation ratio ranging from 33.6 to 74.7% during an isometric knee extension task performed at 20% of MVC, with an almost equal number of participants demonstrating either greater VL activation or greater VM activation. Overall, these results highlight how group data may lead researchers/clinicians to underestimate important

Downloaded from www.physiology.org/journal/jappl by ${individualUser.givenNames} ${individualUser.surname} (109.007.033.126) on August 30, 2018.
Copyright © 2018 American Physiological Society. All rights reserved.

differences between individuals, potentially resulting in the incorrect conclusion that individuals use similar activation strategies.

Importantly, the aforementioned differences between individuals in muscle activation can only be considered as evidence of individual-specific strategies if these strategies persist over time (11). Our findings showed an overall good between-day reliability of muscle activation ratios, which was reflective of robust activation strategies. In addition, the vast majority of studies have reported EMG values from one leg under the basic assumption that muscle activations are similar for both legs. Ounpuu & Winter (29) did not confirm this hypothesis for multiple muscles during gait and concluded that pooled subject data may conceal bilateral differences. In contrast, during a submaximal isometric contraction with fewer degrees of freedom, we observed large significant correlations of the activation ratios between legs ($0.55 < r < 0.75$). Although these correlations do not mean that activation strategies are strictly the same, they confirm that these strategies are consistent between legs, which further supports the hypothesized existence of individual muscle coordination signatures (15). Importantly, the functional consequences of such individual differences in activation strategy require that the muscle torque-generating capacity and its interplay with activation be taken into account.

4.2. Muscle torque-generating capacity and its relationship with activation

To date, hamstring PCSA has been measured mainly in cadavers because of technical limitations related to the measurement of muscle fascicle length *in vivo*, especially for muscles with complex fiber arrangement such as the hamstrings (18, 42, 44). Taking advantage of panoramic ultrasound, we estimated the distribution of PCSA and reported large differences between muscles; the PCSA of BF and SM was similar, while that of ST was consistently smaller (Table 3). Our values concur with those reported from cadavers (12.1%, 46.5% and 41.4% for ST/Hams, SM/Hams, BF/Hams, respectively (42)). These differences in

Downloaded from www.physiology.org/journal/jappl by ${individualUser.givenNames} ${individualUser.surname} (109.007.033.126) on August 30, 2018.
Copyright © 2018 American Physiological Society. All rights reserved.

force-generating capacity can be either compensated or exacerbated at the joint level by different moment arms. Although ST exhibited a longer moment arm (5.7 ± 0.7 cm) than SM (4.8 ± 0.5 cm) and BF (4.6 ± 0.4 cm), the longer moment arm did not completely compensate for its lower torque-generating capacity. Our results highlighted a large variability in torque and force-generating capacity between muscle heads. Importantly, the magnitude of these differences varies greatly between participants.

Previous studies have shown that the activation a muscle receives and its mechanical properties are coupled (12, 14). For instance, Hug et al. (14) showed that the greater the PCSA of VL compared with VM, the stronger the bias of the activation toward VL. Inevitably, this induces a large imbalance of force between the synergist muscles crossing the same joint. In this study, we observed neither positive nor negative correlations between the PCSA and the EMG ratio or between the torque-generating capacity and the EMG ratio. Why our results are different from previous results (14) is unclear. It might be explained by different functional roles of the muscles crossing the knee joint, with the vastii mainly generating torque and the hamstring mainly controlling the direction of the torque (40). It is also possible that the functional consequences of such a coupling would have negative consequences for the non-muscular structures that surround the hamstring muscles. Indeed, the difference in force-generating capacity between VL and VM (for which a coupling was observed) is less than what we observed herein between the heads of the hamstring. As such, a positive correlation between torque-generating capacity and activation of the hamstring would have induced a much larger imbalance of torque than that observed for the *vasti*. However, it is important to note that, even though this positive correlation was not observed, neither was a negative correlation observed, meaning that the differences in torque-generating capacity were not counterbalanced by opposite differences in activation. This has led to a wide range of individual torque-sharing strategies.

Downloaded from www.physiology.org/journal/jappl by ${individualUser.givenNames} ${individualUser.surname} (109.007.033.126) on August 30, 2018.
Copyright © 2018 American Physiological Society. All rights reserved.

4.3. Individual-specific torque-sharing strategies

The muscle heads displayed differences in torque contribution, e.g., BF/Hams, SM/Hams and ST/Hams accounted for 37.9 ± 10.1% (range: 20.2–54.8%), 43.9 ± 9.8% (range: 28.3–63.7%) and 18.3 ± 6.7% (range: 9.1–39.9%) of the torque-generating capacity, respectively (Fig. 3A). Interestingly, comparable ratios of force (without considering the moment arm) were estimated by a musculoskeletal model during the stance phase of high speed running (6). Beyond the between-muscle differences, we believe that the description of the individual-specific torque-sharing strategies is the main result of this study (Fig. 3A). For example, the torque produced by BF and ST in participant #1 accounted for 54.8% and 16.8% of the total torque required to reach the target of 20% of the MVC torque. To complete the same task, participant #23 generated 24.2% of the total torque with BF and 39.9% with ST. These individual differences resulted from interindividual variability of the distribution of both activation and torque-generating capacity. Even though interindividual variability of muscle activation is logically larger at relatively low contraction intensities (14), as studied here, the absolute between-muscle differences in torque would be greater at higher intensities, despite a more balanced activation.

The interindividual variability of muscle coordination strategies may support the idea that individuals can perform the task with a range of *good-enough strategies* (23), rather than requiring an iterative optimization to a specific strategy. In short, following a trial-and-error process, nervous system saves successful programs that can be recalled when facing a similar task (23). Thus, the contraction history may influence both the number of motor programs available to complete the task and the efficiency of those programs (32). Such individual differences might have functional consequences for the musculoskeletal system (15) and might affect motor performance (34, 35).

Downloaded from www.physiology.org/journal/jappl by ${individualUser.givenNames} ${individualUser.surname} (109.007.033.126) on August 30, 2018.
Copyright © 2018 American Physiological Society. All rights reserved.

4.4. Distribution of muscle activation influences muscle performance

The observed individual differences in the distribution of muscle activation might have important functional consequences with some strategies being less effective. For example, if one muscle is activated to a greater extent than required by the task, which is inevitably the case when activation among the synergists is imbalanced, its metabolic demand would be higher and, therefore, fatigue would develop sooner (39). Fatigue models predict that the task is interrupted, or force is decreased, to prevent physiological failure (26, 28). Therefore, it is possible that the first muscle that reaches this "threshold" would limit the overall performance. In this way, Prilutsky and Zatsiorsky (31) suggested that fatigue may be minimized if stress is more evenly distributed among muscles. Our results support the aforementioned hypothesis. To begin, although it is difficult to interpret the change in EMG amplitude as a change in activation during a fatiguing task (8, 13), the ratios of EMG amplitudes did not vary during the fatiguing task, allowing us to assume that the activation strategies persisted throughout the task. It was important to test this (albeit indirectly), because a change in activation strategy with fatigue had already been reported in some studies (2, 17), but not in others (33). Second, we estimated the imbalance of activation among the muscle heads by calculating the standard deviation of the EMG amplitude. Note that we found a positive correlation between the magnitude of the standard deviation and the highest EMG amplitude value among muscle heads ($r = 0.50$ [$P = 0.002$] and $r = 0.60$ [$P < 0.001$] for the dominant leg and the non-dominant leg, respectively). This confirmed our assumption that the more imbalanced the activation between the muscle heads, the higher the activation of the most activated muscle. Third, and more importantly, we observed a strong (dominant leg) or moderate (non-dominant leg) negative correlation between the standard deviation values and the time to exhaustion (Fig. 4). This indicates that the larger the difference in activation

Downloaded from www.physiology.org/journal/jappl by ${individualUser.givenNames} ${individualUser.surname} (109.007.033.126) on August 30, 2018.
Copyright © 2018 American Physiological Society. All rights reserved.

between the muscle heads, the shorter the time to exhaustion. Although the finding that muscle activation strategies influence endurance performance is novel, one should keep in mind that other factors, such as muscle architecture (3), muscle typology and training level (4), are known to affect endurance performance. This multifactorial origin of endurance performance may explain why the coefficients of correlation are not higher. Even so, we believe that our results support the concept that individual coordination strategies may have functional consequences, such as an effect on motor performance. To the best of our knowledge, this is a novel finding. It has potential importance for hamstring strain injuries, which have been argued to be related to fatigability and the associated compensation between synergists (34, 35).

4.5. Methodological considerations

Some methodological considerations should be kept in mind when interpreting the present data. First, we used surface EMG amplitude as a surrogate for muscle activation. Therefore, it is important to consider the factors that could influence the relationship between EMG amplitude and muscle activation. Among these factors, we believe that crosstalk and the normalization procedure are the most important. Although EMG signals from the hamstring might be affected by crosstalk, we systematically used B-mode ultrasound to place the electrodes over the muscle of interest, away from the borders where signal contamination is strongest. This procedure allowed us to distinguish between the SM and ST muscles, which are difficult to differentiate using palpation (10). It is important to note that if we run the same analysis considering only the medial (MH, i.e. SM + ST) and lateral hamstrings (LH, i.e. BF), there is still no correlation between LH/(LH+MH) activation ratio and LH/(LH+MH) torque-generating capacity ratio. Taken together with the consistency of the EMG data between days and between legs, we are confident that crosstalk did not interfere with our main conclusions.

Downloaded from www.physiology.org/journal/jappl by ${individualUser.givenNames} ${individualUser.surname} (109.007.033.126) on August 30, 2018.
Copyright © 2018 American Physiological Society. All rights reserved.

Also, the accuracy of between-muscle and between-participant comparisons lies in the truly maximal voluntary activation during the maximal contraction used to normalize EMG amplitude. Using the twitch interpolation method (38), previous studies have reported that young healthy participants (similar to those in our experiment) are able to achieve near-complete activation of their hamstrings (97.1 ± 2.2% (24) and 98.7 ± 1.3% (20)). Therefore, the EMG amplitude measured during maximal contractions likely represents the true maximal muscle activation.

Second, we estimated muscle torque-generating capacity from PCSA and the moment arm measured at rest. Even though fascicles shorten during contraction, therefore affecting PCSA (27), previous works demonstrated that PCSA measured at rest is as strongly related with muscle strength as PCSA measured during MVC (25). It is also possible that muscle contraction induced slight changes in both the line of action and the joint center of rotation, leading to modification of muscle moment arm. To the best of our knowledge, such changes have not been reported. Although it is possible that such alterations may occur, their magnitude would have remained low during such a low intensity isometric contraction, i.e. 20% MVC.

Finally, although we considered two important mechanical factors (i.e., PCSA and moment arm) that influence the torque-generating capacity during such an isometric task, we did not consider either the specific tension or the individual muscle force–length relationship. However, to date, no experimental technique is available to measure these mechanical factors accurately. In addition, specific tension varies only marginally between muscles with similar fiber type composition (30, 43), especially at low contraction intensities during which slow fibers are recruited preferentially. Therefore, we believe that considering specific tension would not have affected the between-muscle differences in torque production. In addition, estimating the between-muscles differences in torque-generating capacity during an isometric

Downloaded from www.physiology.org/journal/jappl by ${individualUser.givenNames} ${individualUser.surname} (109.007.033.126) on August 30, 2018.
Copyright © 2018 American Physiological Society. All rights reserved.

552 task should take into account possible between-muscles differences in the shape of the force–
553 length relationship. Although such a relationship cannot be determined for each individual
554 muscle head, the fascicle lengths we measured near the optimal angle were similar to the
555 optimal length previously reported from cadaver preparations (e.g. 10.7 ± 1.4 cm vs. 11.0 ±
556 2.1 cm for BFsh in Ward (42)). Therefore, it is reasonable to consider that each of the three
557 heads did operated at a similar relative length.
558
559 **5. CONCLUSIONS**
560 Both the distribution of activation and the distribution of torque-generating capacity varied
561 greatly between individuals. In the absence of a negative coupling between activation and
562 torque-generating capacity, a wide range of torque-sharing strategies was observed. To the
563 best of our knowledge, this is the first study to show a relationship between individual-
564 specific activation strategies and performance during an endurance task. Overall, this study
565 provides new insight into the coordination between the heads of the hamstring during
566 submaximal contractions. The observed variability between individuals provide a basis from
567 which to consider muscle coordination strategies as an intrinsic risk factor for hamstring
568 strain injury.
569

Downloaded from www.physiology.org/journal/jappl by ${individualUser.givenNames} ${individualUser.surname} (109.007.033.126) on August 30, 2018.
Copyright © 2018 American Physiological Society. All rights reserved.

ACKNOWLEDGMENTS:

The authors thank the technicians from the lab Imagerie par Résonance Magnétique Médicale et Multi-modalités (IR4M-UMR8081), for their assistance with MRI data collection.

GRANTS:

S. Avrillon was supported by a scholarship funded by the French Ministry of Research. F. Hug was supported by a fellowship from the Institut Universitaire de France (IUF).

DISCLOSURES:

No conflicts of interest, financial or otherwise, are declared by the authors. Authors declare that they have no conflicts of interest relevant to the content of this original research article.

Downloaded from www.physiology.org/journal/jappl by ${individualUser.givenNames} ${individualUser.surname} (109.007.033.126) on August 30, 2018.
Copyright © 2018 American Physiological Society. All rights reserved.

581 TABLES:

582

583 Table 1. RMS EMG amplitude of the biceps femoris (BF) semimembranosus (SM) and
584 semitendinosus (ST) muscles during the submaximal isometric knee extension task. ICC,
585 intra-class coefficient correlation; TE, typical error. Values are means ± SD.

586

	DOMINANT LEG			**NON-DOMINANT LEG**			**MAIN EFFECT**		
	BF (% max)	SM (% max)	ST (% max)	BF (% max)	SM (% max)	ST (% max)	Leg	Muscle	Interaction
DAY 1	13.0 ± 4.4	14.6 ± 4.7	11.8 ± 5.4	12.7 ± 3.3	14.1 ± 4.1	12.2 ± 3.6			
DAY 2	13.2 ± 4.8	15.0 ± 4.8	12.8 ± 5.5	11.8 ± 3.8	14.6 ± 4.7	11.4 ± 5.3			
AVERAGE	13.1 ± 4.3	14.8 ± 4.4[a]	12.3 ± 5.2[b]	12.2 ± 3.0	14.3 ± 3.9[a]	11.8 ± 3.9[b]	P = 0.34	**P = 0.036**	P = 0.83
ICC	0.74	0.74	0.85	0.45	0.59	0.51			
TE	2.4	2.5	2.2	2.7	2.9	3.2			

587 Superscript letters denote significant differences with: [a]ST, [b]SM.

588

589 Table 2. Activation ratios between the heads of the hamstring muscle group. ICC, intra-class
590 coefficient correlation; TE, typical error. Values are means ± SD.

591

	DOMINANT LEG			**NON-DOMINANT LEG**		
	BF/Hams (%)	SM/Hams (%)	ST/Hams (%)	BF/Hams (%)	SM/Hams (%)	ST/Hams (%)
Day 1	33.4 ± 8.0	37.3 ± 7.8	29.3 ± 7.4	32.6 ± 7.7	36.2 ± 8.7	31.1 ± 7.0
Day 2	32.7 ± 8.6	36.8 ± 7.4	30.5 ± 7.6	31.9 ± 9.2	38.8 ± 8.2	29.3 ± 9.6
ICC	0.77	0.88	0.68	0.72	0.75	0.57
TE	4.1	2.7	4.4	4.6	4.4	5.6

592

593

594 Table 3. Morphological and architectural data for the biceps femoris long head (BFlh), short
595 head (BFsh), semimembranosus (SM) and semitendinosus (ST) muscles. fl,

Downloaded from www.physiology.org/journal/jappl by ${individualUser.givenNames} ${individualUser.surname} (109.007.033.126) on August 30, 2018.
Copyright © 2018 American Physiological Society. All rights reserved.

596 fascicle length; PA, pennation angle; PCSA, physiological cross-sectional area; TGC, torque-

597 generating capacity. Values are means ± SD.

598

	DOMINANT LEG				NON-DOMINANT LEG				MAIN EFFECT		
	BFsh	BFlh	SM	ST	BFsh	BFlh	SM	ST	Leg	Muscle	Interaction
VOLUME (CM^3)	86.3 ± 37.6^{bcd}	184.6 ± 41.6^{ac}	207.5 ± 56.7^{abd}	173.4 ± 67.3^{ac}	85.2 ± 34.7^{bcd}	178.2 ± 47.6 ^{c}	207.7 ± 53.7^{abd}	178.0 ± 67.5 ^{c}	P = 0.71	**P < 0.001**	P = 0.24
FL (CM)	10.7 ± 1.4^{d}	12.1 ± 1.7^{cd}	8.9 ± 1.4^{bd}	17.2 ± 4.4^{abc}	10.8 ± 1.2^{d}	11.9 ± 1.6^{d}	9.0 ± 1.2^{bd}	17.1 ± 3.9^{abc}	P = 0.80	**P < 0.001**	P = 0.86
PA (°)	12.4 ± 2.4^{bc}	9.0 ± 1.6^{ac}	10.7 ± 2.0^{ab}		11.9 ± 2.8^{bc}	9.3 ± 1.9^{ac}	11.1 ± 1.8^{ab}		P = 0.89	**P < 0.001**	P = 0.42
PCSA (CM^2)	7.9 ± 3.3^{bcd}	15.2 ± 3.6^{acd}	23.4 ± 7.6^{abd}	10.2 ± 3.9^{abc}	7.8 ± 3.1^{bcd}	15.0 ± 4.1^{acd}	22.9 ± 6.0^{abd}	10.7 ± 3.8^{abc}	P = 0.74	**P < 0.001**	P = 0.69
MOMENT ARM (CM)	4.6 ± 0.4^{bc}		4.8 ± 0.5^{ac}	5.7 ± 0.7^{ab}	4.5 ± 0.4^{bc}		4.8 ± 0.4^{ac}	5.8 ± 0.6^{ab}	P = 0.36	**P < 0.001**	P = 0.19
TGC	107.3 ± 34.8^{c}		113.3 ± 44.7^{c}	60.2 ± 27.9^{ab}	104.5 ± 34.1^{c}		110.1 ± 33.0^{c}	63.2 ± 26.3^{ab}	P = 0.73	**P < 0.001**	P = 0.50

599 Letters in superscript denotes significant differences with: ^{a}BFsh, ^{b}BFlh, ^{c}SM, ^{d}ST.

Downloaded from www.physiology.org/journal/jappl by ${individualUser.givenNames} ${individualUser.surname} (109.007.033.126) on August 30, 2018.
Copyright © 2018 American Physiological Society. All rights reserved.

FIGURE CAPTIONS:

Fig. 1. Individual example of estimating the torque-generating capacity from MRI and ultrasound images. A. Muscle volume reconstruction of semitendinosus (ST), semimembranosus (SM) biceps femoris long head (BFlh) and short head (BFsh). B. Reconstruction of musculotendon path after manual segmentation to measure the moment arm (i.e., the shortest distance between the joint center and the musculotendon path). C. Panoramic US image of SM to determine fascicle length. Muscle fascicles were imaged through a longitudinal scan performed in the fascicle's plane. Particular care was taken to measure fully visible fascicles in a region of interest including clear aponeuroses.

Fig. 2. Box charts depicting mean values (line) ± one standard deviation (box) and individual values (scatters) of EMG amplitude (A) and torque-generating capacity (B). EMG amplitude referred to normalized EMG RMS values. Group distribution is given for the ratio of muscle activation (A) and the ratio of torque-generating capacity (B).

Fig. 3. (A) Group distribution of the torque index ratio. The correlations for BF, SM and ST (B) indicate that torque-sharing strategies are similar between legs. The solid line represents equal torque generation between legs.

Fig. 4. Correlations between the imbalance of muscle activation and the time to task failure. The imbalance of activation was assessed through the standard deviation of normalized RMS EMG across the muscle heads. These correlations indicate that the larger the imbalance in muscle activation among synergists, the sooner failure occurs in the endurance task. Note that

Downloaded from www.physiology.org/journal/jappl by ${individualUser.givenNames} ${individualUser.surname} (109.007.033.126) on August 30, 2018.
Copyright © 2018 American Physiological Society. All rights reserved.

the coefficient of correlation was even higher when the two participants who exhibited the longest times to exhaustion are not considered.

Downloaded from www.physiology.org/journal/jappl by ${individualUser.givenNames} ${individualUser.surname} (109.007.033.126) on August 30, 2018.
Copyright © 2018 American Physiological Society. All rights reserved.

627 REFERENCES

628 1. **Adkins AN, Franks PW, and Murray WM**. Demonstration of extended field-of-
629 view ultrasound's potential to increase the pool of muscles for which in vivo fascicle length is
630 measurable. *J Biomech* 2017.
631 2. **Akima H, Foley JM, Prior BM, Dudley GA, and Meyer RA**. Vastus lateralis
632 fatigue alters recruitment of musculus quadriceps femoris in humans. *J Appl Physiol (1985)*
633 92: 679-684, 2002.
634 3. **Biewener AA**. Locomotion as an emergent property of muscle contractile dynamics. *J*
635 *Exp Biol* 219: 285-294, 2016.
636 4. **Cairns SP, Knicker AJ, Thompson MW, and Sjogaard G**. Evaluation of models
637 used to study neuromuscular fatigue. *Exerc Sport Sci Rev* 33: 9-16, 2005.
638 5. **Cappozzo A, Catani F, Della Croce U, and Leardini A**. Position and orientation in
639 space of bones during movement: anatomical frame definition and determination. *Clin*
640 *Biomech* 10: 171-178, 1995.
641 6. **Chumanov ES, Heiderscheit BC, and Thelen DG**. Hamstring musculotendon
642 dynamics during stance and swing phases of high-speed running. *Med Sci Sports Exerc* 43:
643 525-532, 2011.
644 7. **Cohen J**. Differences between Correlation Coefficients. In: *Statistical Power Analysis*
645 *for the Behavioral Sciences (Revised Edition)*Academic Press, 1977, p. 109-143.
646 8. **Farina D, Merletti R, and Stegeman DF**. Biophysics of the Generation of EMG
647 Signals. In: *Electromyography*John Wiley & Sons, Inc., 2005, p. 81-105.
648 9. **Garrett WE, Jr., Califf JC, and Bassett FH, 3rd**. Histochemical correlates of
649 hamstring injuries. *Am J Sports Med* 12: 98-103, 1984.
650 10. **Hermens HJ, Freriks K, Disselhorst-Klug C, and Rau G**. Development of
651 recommendations for SEMG sensors and sensor placement procedures. *J Electromyogr*
652 *Kinesiol* 2000.
653 11. **Horst F, Mildner M, and Schollhorn WI**. One-year persistence of individual gait
654 patterns identified in a follow-up study - A call for individualised diagnose and therapy. *Gait*
655 *Posture* 58: 476-480, 2017.
656 12. **Hudson AL, Taylor JL, Gandevia SC, and Butler JE**. Coupling between
657 mechanical and neural behaviour in the human first dorsal interosseous muscle. *J Physiol* 587:
658 917-925, 2009.
659 13. **Hug F**. Can muscle coordination be precisely studied by surface electromyography? *J*
660 *Electromyogr Kinesiol* 21: 1-12, 2011.
661 14. **Hug F, Goupille C, Baum D, Raiteri BJ, Hodges PW, and Tucker K**. Nature of the
662 coupling between neural drive and force-generating capacity in the human quadriceps muscle.
663 *Proc Biol Sci* 282: 2015.
664 15. **Hug F, and Tucker K**. Muscle Coordination and the Development of
665 Musculoskeletal Disorders. *Exerc Sport Sci Rev* 2017.
666 16. **Hunter SK, Duchateau J, and Enoka RM**. Muscle Fatigue and the Mechanisms of
667 Task Failure. *Med Sci Sports Exerc* 2004.
668 17. **Hunter SK, and Enoka RM**. Changes in muscle activation can prolong the
669 endurance time of a submaximal isometric contraction in humans. *J Appl Physiol (1985)* 94:
670 108-118, 2003.
671 18. **Kellis E, Galanis N, Natsis K, and Kapetanos G**. Muscle architecture variations
672 along the human semitendinosus and biceps femoris (long head) length. *J Electromyogr*
673 *Kinesiol* 20: 1237-1243, 2010.

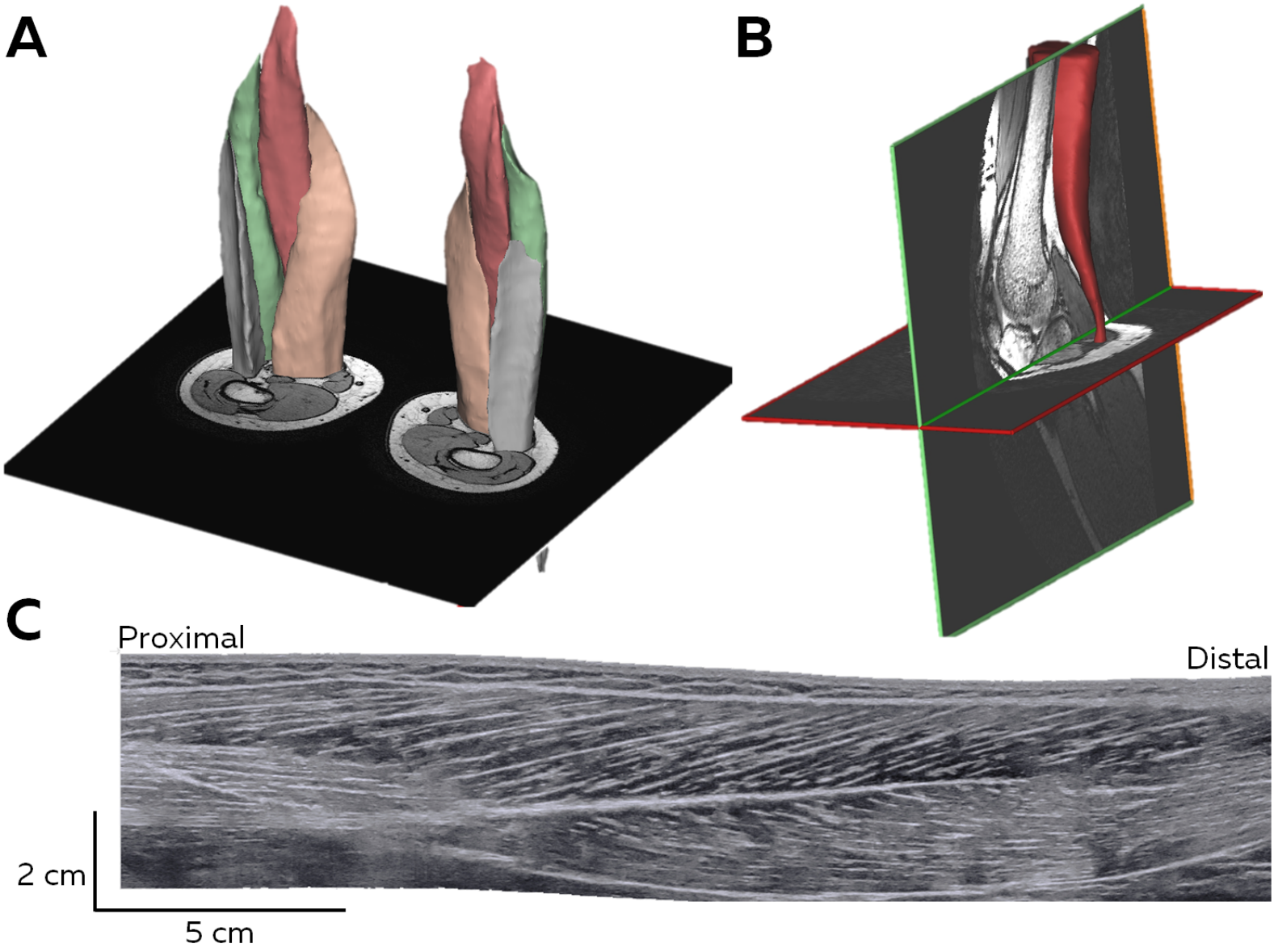
Downloaded from www.physiology.org/journal/jappl by ${individualUser.givenNames} ${individualUser.surname} (109.007.033.126) on August 30, 2018.
Copyright © 2018 American Physiological Society. All rights reserved.

19. **Kilgallon M, Donnelly AE, and Shafat A**. Progressive resistance training temporarily alters hamstring torque-angle relationship. *Scan J Med Sci Sports* 17: 18-24, 2007.
20. **Kirk EA, and Rice CL**. Contractile function and motor unit firing rates of the human hamstrings. *J Neurophysiol* 117: 243-250, 2017.
21. **Lacourpaille L, Nordez A, and Hug F**. The nervous system does not compensate for an acute change in the balance of passive force between synergist muscles. *J Exp Biol* 2017.
22. **Lieber RL, and Ward SR**. Skeletal muscle design to meet functional demands. *Philos Trans R Soc Lond B Biol Sci* 366: 1466-1476, 2011.
23. **Loeb GE**. Optimal isn't good enough. *Biol Cybern* 106: 757-765, 2012.
24. **Marshall PW, Lovell R, Jeppesen GK, Andersen K, and Siegler JC**. Hamstring muscle fatigue and central motor output during a simulated soccer match. *PLoS One* 9: e102753, 2014.
25. **Massey G, Evangelidis P, and Folland J**. Influence of contractile force on the architecture and morphology of the quadriceps femoris. *Exp Physiol* 100: 1342-1351, 2015.
26. **Millet GY**. Can neuromuscular fatigue explain running strategies and performance in ultra-marathons?: the flush model. *Sports Med* 41: 489-506, 2011.
27. **Narici MV, Binzoni T, Hiltbrand E, Fasel J, Terrier F, and Cerretelli P**. In vivo human gastrocnemius architecture with changing joint angle at rest and during graded isometric contraction. *J Physiol* 496 (Pt 1): 287-297, 1996.
28. **Noakes TD, and St Clair Gibson A**. Logical limitations to the "catastrophe" models of fatigue during exercise in humans. *Br J Sports Med* 38: 648-649, 2004.
29. **Ounpuu S, and Winter DA**. Bilateral electromyographical analysis of the lower limbs during walking in normal adults. *Electroencephalogr Clin Neurophysiol* 72: 429-438, 1989.
30. **Powell PL, Roy RR, Kanim P, Bello MA, and Edgerton VR**. Predictability of skeletal muscle tension from architectural determinations in guinea pig hindlimbs. *J Appl Physiol Respir Environ Exerc Physiol.* 57: 1715-1721, 1984.
31. **Prilutsky BI, and Zatsiorsky VM**. Optimization-based models of muscle coordination. *Exerc Sport Sci Rev* 30: 32-38, 2002.
32. **Ranganathan R, Wieser J, Mosier KM, Mussa-Ivaldi FA, and Scheidt RA**. Learning redundant motor tasks with and without overlapping dimensions: facilitation and interference effects. *J Neurosci* 34: 8289-8299, 2014.
33. **Rudroff T, Christou EA, Poston B, Bojsen-Moller J, and Enoka RM**. Time to failure of a sustained contraction is predicted by target torque and initial electromyographic bursts in elbow flexor muscles. *Muscle Nerve* 35: 657-666, 2007.
34. **Schuermans J, Van Tiggelen D, Danneels L, and Witvrouw E**. Biceps femoris and semitendinosus--teammates or competitors? New insights into hamstring injury mechanisms in male football players: a muscle functional MRI study. *Br J Sports Med* 48: 1599-1606, 2014.
35. **Schuermans J, Van Tiggelen D, Danneels L, and Witvrouw E**. Susceptibility to Hamstring Injuries in Soccer: A Prospective Study Using Muscle Functional Magnetic Resonance Imaging. *Am J Sports Med* 2016.
36. **Seymore KD, Domire ZJ, DeVita P, Rider PM, and Kulas AS**. The effect of Nordic hamstring strength training on muscle architecture, stiffness, and strength. *Eur J Appl Physiol* 117: 943-953, 2017.
37. **Spoor CW, and van Leeuwen JL**. Knee muscle moment arms from MRI and from tendon travel. *J Biomech* 25: 201-206, 1992.

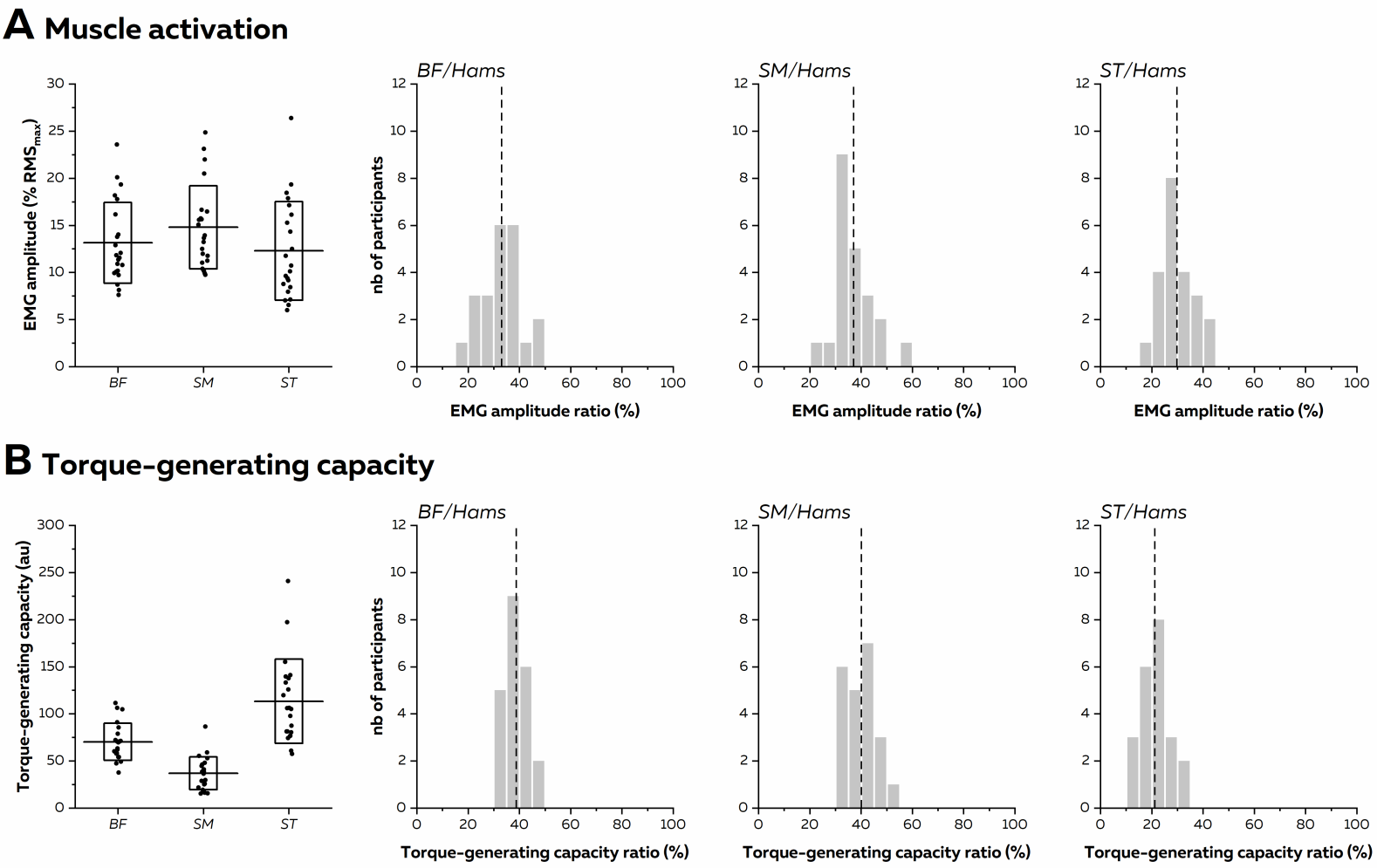
Downloaded from www.physiology.org/journal/jappl by ${individualUser.givenNames} ${individualUser.surname} (109.007.033.126) on August 30, 2018.
Copyright © 2018 American Physiological Society. All rights reserved.

38. **Todd G, Taylor JL, and Gandevia SC**. Reproducible measurement of voluntary activation of human elbow flexors with motor cortical stimulation. *J Appl Physiol (1985)* 97: 236-242, 2004.
39. **Tsianos GA, Rustin C, and Loeb GE**. Mammalian muscle model for predicting force and energetics during physiological behaviors. *IEEE Trans Neural Syst Rehabil Eng* 20: 117-133, 2012.
40. **van Ingen Schenau GJ, Dorssers WM, Welter TG, Beelen A, de Groot G, and Jacobs R**. The control of mono-articular muscles in multijoint leg extensions in man. *J Physiol* 484 (Pt 1): 247-254, 1995.
41. **Visser JJ, Hoogkamer JE, Bobbert MF, and Huijing PA**. Length and moment arm of human leg muscles as a function of knee and hip-joint angles. *Eur j appl physiol occup physiol* 61: 453-460, 1990.
42. **Ward SR, Eng CM, Smallwood LH, and Lieber RL**. Are current measurements of lower extremity muscle architecture accurate? *Clin Orthop Relat Res* 467: 1074-1082, 2009.
43. **Wickiewicz TL, Roy RR, Powell PL, and Edgerton VR**. Muscle Architecture of the Human Lower Limb. *Clin Orthop Relat Res* 179: 275???283, 1983.
44. **Woodley SJ, and Mercer SR**. Hamstring muscles: architecture and innervation. *Cells Tissues Organs* 179: 125-141, 2005.

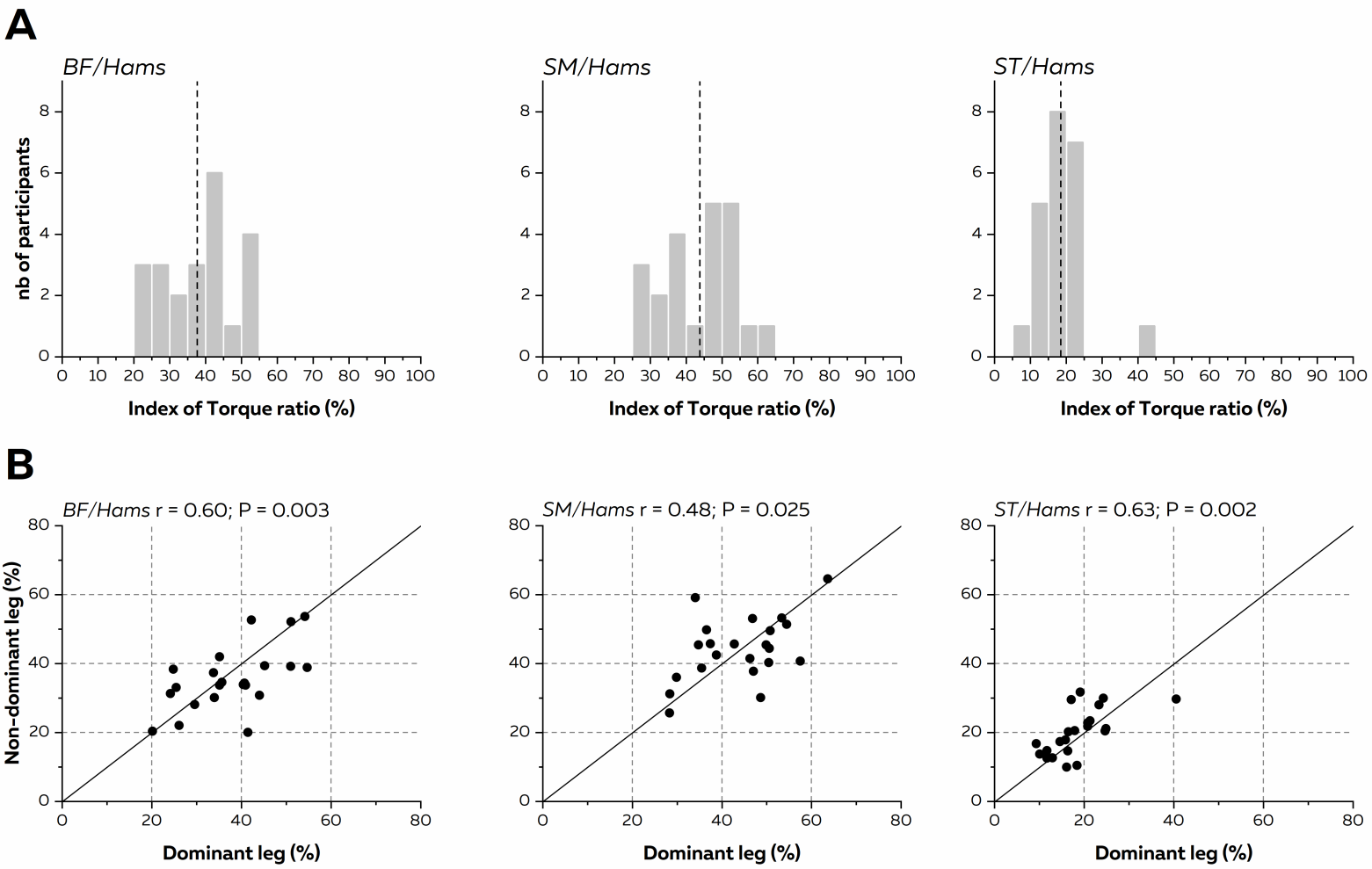
Downloaded from www.physiology.org/journal/jappl by ${individualUser.givenNames} ${individualUser.surname} (109.007.033.126) on August 30, 2018.
Copyright © 2018 American Physiological Society. All rights reserved.



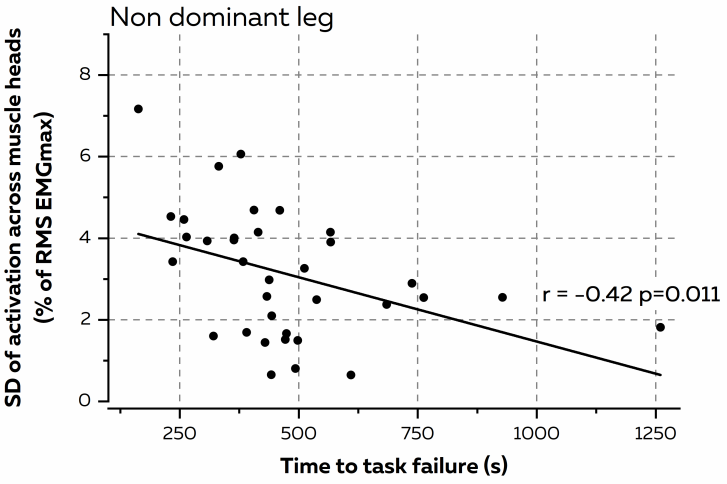
Downloaded from www.physiology.org/journal/jappl by ${individualUser.givenNames} ${individualUser.surname} (109.007.033.126) on August 30, 2018.
Copyright © 2018 American Physiological Society. All rights reserved.

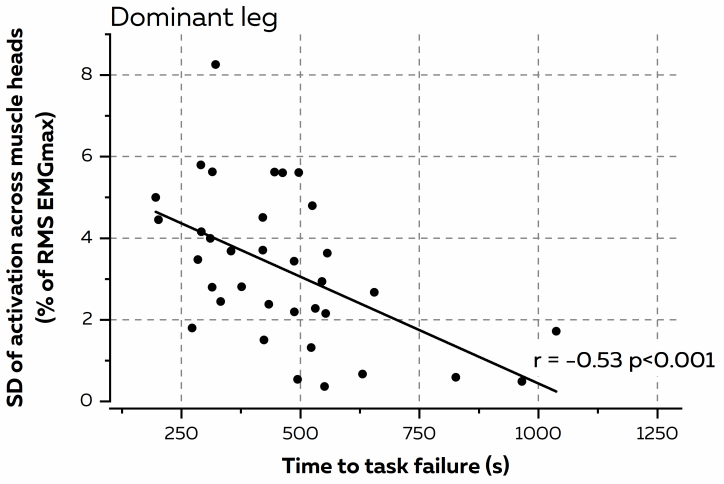


Downloaded from www.physiology.org/journal/jappl by ${individualUser.givenNames} ${individualUser.surname} (109.007.033.126) on August 30, 2018.
Copyright © 2018 American Physiological Society. All rights reserved.



Downloaded from www.physiology.org/journal/jappl by ${individualUser.givenNames} ${individualUser.surname} (109.007.033.126) on August 30, 2018.
Copyright © 2018 American Physiological Society. All rights reserved.





Downloaded from www.physiology.org/journal/jappl by ${individualUser.givenNames} ${individualUser.surname} (109.007.033.126) on August 30, 2018.
Copyright © 2018 American Physiological Society. All rights reserved.